Iterative Detection Assisted Cooperative Vehicular Ad Hoc Networking Using Differential Linear Dispersion Coding

S. Sugiura[⋆] **and L. Hanzo**[†]

[⋆,†]School of ECS, University of Southampton, SO17 1BJ, UK, Tel: +44-23-8059-3125, Fax: +44-23-8059-4508

Email: {ss07r,lh}@ecs.soton.ac.uk, http://www-mobile.ecs.soton.ac.uk

[⋆]TOYOTA Central R&D Labs., Inc., Aichi, 480-1192, Japan, Tel: +81-561-71-7163, Fax: +81-561-63-5258

Email: sugiura@mosk.tytlabs.co.jp, http://www.tytlabs.co.jp/eindex.html

***Abstract*— In this paper, we propose a Differential Linear Dispersion Coded (DLDC) cooperative transmission scheme suitable for Vehicular Ad Hoc NETworks (VANETs), which facilitates striking a flexible diversity-multiplexing gain tradeoff without requiring channel estimation both at the cooperating nodes and at the destination node. More specifically, DLDC encoding is employed by the source transmitter for broadcasting the source information to the relays, while an LDC-based *amplify-and-forward* relaying scheme is used at the relays. The proposed technique allows each relay to decide, whether it joins the cooperating cluster without any negotiations with the other nodes. The destination's receiver detects the DLDC-encoded symbols using a low-complex detection algorithm, rather than an exhaustive Maximum Likelihood (ML) search. Based on the serial-concatenated turbo coding principle, the source node is constituted by the outer channel encoder, a Unity Rate Convolutional (URC) encoder and the DLDC-based mapper. The destination's receiver iteratively decodes the received signals, exchanging soft information between the DLDC demapper, the URC decoder and the channel decoder. We demonstrate that the proposed cooperative scheme attained a BER of 10^{-5} within 2.8 dB of the capacity-dependent maximum achievable rate and significantly outperformed the classic MIMOs suffering from the correlated shadow fading of the co-located elements imposed by large-bodied vehicles. We also investigate the effect of different source-relay channels, including perfect, Additive White Gaussian Noise (AWGN), Rician and Rayleigh channels. We conclude by demonstrating that the introduction of an appropriate source-relay SNR threshold for deciding as to whether to actively engage in cooperation improves the achievable performance.**

I. Introduction

Vehicular Ad hoc NETworks (VANETs), supporting both Vehicle-to-Vehicle (V2V) and Vehicle-to-Infrastructure (V2I) communications, have been extensively investigated in diverse applications [1]. Although vehicular safety applications are of special interest owing to the reduction of the number of the traffic accidents, for example, achieving the required high reliability in hostile VANET propagation environments necessitates further research due to rapid topology changes and shadowing-induced large-scale fading, especially in the absence of central coordination.

As a result of intensive studies of Multiple-Input Multiple-Output (MIMO) techniques over the last decade [2], the family of Space-Time Codes (STCs) [3]-[4] provides substantial diversity gains without any bandwidth extension. Linear Dispersion Codes (LDCs) [5], [6] and Differential LDCs (DLDCs) [7] were designed for striking a flexible diversity-multiplexing gain tradeoff for an arbitrary number of transmit and receive antennas, when using diverse modulation constellation sizes. However, the antenna elements of collocated MIMO systems suffer from correlated fading imposed by the shadowing effect of large-bodied vehicles [8] or by the extra attenuation of street corners [9] in VANET environments.

Recently, cooperative space-time diversity schemes were proposed [10]-[12], where a collection of mobile nodes using a single antenna element act in a concerted manner as an antenna array, in order to combat the above-mentioned limitations of the collocated MIMOs. More specifically, the typically large separation of the distributed antenna elements enables us to achieve the best attainable diversity gain of uncorrelated elements, even in the face of large-scale fading. However, attaining cooperative space-time diversity in VANETs imposes further challenges in terms of their practical implementation. Firstly, the lack of a central coordinating node makes the information sharing between the cooperating nodes quite a challenge, which may require a sophisticated transmission procedure at the relays. The next challenge is the acquisition of accurate channel estimation for both the source-relay channel and/or for the relay-destination channel for the rapidly changing topology of vehicles, which may travel at speeds in excess of 100 km/h. Additionally, in such a dynamic-topology environment it is desirable for the relays to join or disjoin the cooperating cluster without any negotiation with either the source, the other relays or the destination for the above-mentioned reasons. Recently, a sophisticated differential distributed STC scheme was developed [13], which was motivated by the unitary differential space-time modulation philosophy [4] and by the LDC-based relaying technique of [12], where no channel information was required at the relays or at the destination. This scheme pre-assigned a set of unitary matrices to the source, while assigning appropriate dispersion matrices to the relays, depending on the number of the relays. Although an arbitrary number of relays may be supported by this scheme, the resultant decoding complexity becomes high, except for Alamouti's code supporting $M = 2$ relays.

Against this background, the novel contributions of this paper are as follows. We propose a DLDC-encoded cooperative transmission scheme suitable for VANETs, which is capable of striking a flexible balance between the achievable diversity and multiplexing gain without channel estimation at the relays. Furthermore, our LDC-based *amplify-and-forward* relaying scheme allows the relays to decide autonomously based on the received SNR, whether to join or disjoin a cooperating cluster. In addition, the destination can detect the DLDC-encoded symbols using an efficient low-complexity detection algorithm, rather than the high-complexity exhaustive search technique of [13]. Another contribution of this paper is that a three-stage turbo coding scheme is applied in the proposed cooperative scheme. EXtrinsic Information Transfer (EXIT) chart analysis is employed to investigate the characteristics of the iterative detectors and to determine the maximum achievable rate of our system. We also investigate the effect of both perfect source-relay channels and of different source-relay channels, such as Rayleigh fading, Rician fading, Additive White Gaussian Noise (AWGN) channels operating at different source-relay SNRs. Moreover, the effects of the spontaneous cooperation of relays are demonstrated in the specific scenario, where each relay experiences different source-relay SNRs.

The financial support of the EU under the auspices of the Optimix project and also that of the EPSRC is thankfully acknowledged.

978-1-4244-2515-0/09/$25.00 ©2009 IEEE

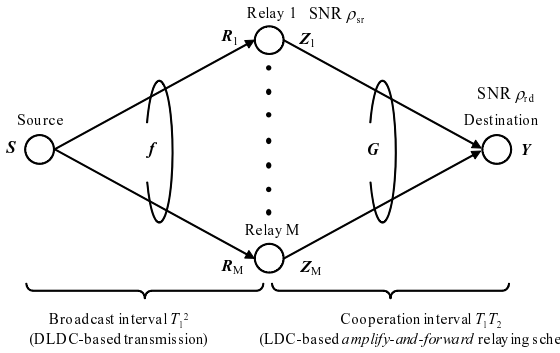

Fig. 1. Schematic of the proposed cooperative system employing a DLDC-based broadcast phase and an LDC-based cooperation phase.

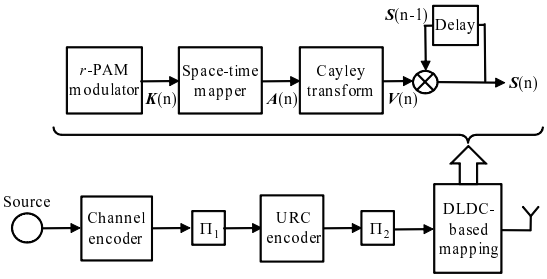

Fig. 2. Source node structure.

II. System Description

Consider the twin-layer cooperative wireless network shown in Fig. 1, which is composed of a source node, M relay nodes and a single destination, where each of the source and relay nodes has a single antenna, while the destination's receiver has N antennas. Here, we consider the VANET scenario, where a collection of vehicles forms a cooperating cluster and one of them acts as a cluster-head transmitting to the other vehicles or to the fixed Base Station (BS) infrastructure. This cluster-head node is also referred to as the source in this paper. It is assumed that a decentralized Time Division Multiple Access (TDMA) protocol, reminiscent of that proposed in [14], is used and that the timing of the cooperating relays is perfectly symbol-synchronized. We also assume that each node is operated in a half-duplex mode, either receiving or transmitting in a given time slot.

During the broadcast phase of Fig. 1 the source broadcasts the DLDC-encoded space-time blocks $\boldsymbol{S}(n) \in \mathcal{C}^{T_1 \times T_1}$ to the relay nodes, where n is the block index. The source node's transmitter structure is detailed in Fig. 2, where the source bits are first channel-encoded and interleaved by the outer interleaver Π_1. Then the interleaved bits are encoded by a Unity Rate Convolutional (URC) encoder and interleved again by the inner interleaver Π_2. Then the interleaved bits are modulated to r-bit Puls Amplitude Modulation (PAM) symbols $\boldsymbol{K}(n) = [s_1(n), \cdots, s_Q(n)]^T$ and then the modulated symbols $\boldsymbol{K}(n)$ are further mapped to a unitary matrix $\boldsymbol{V}(n)$ by using the unitary Cayley transform, which is given by [7]

$$\boldsymbol{V}(n) = [\boldsymbol{I} - j\boldsymbol{A}(n)][\boldsymbol{I} + j\boldsymbol{A}(n)]^{-1} \tag{1}$$

with

$$\boldsymbol{A}(n) = \sum_{q=1}^{Q} s_q(n)\boldsymbol{A}_q, \tag{2}$$

where $\boldsymbol{I}$ is the identity matrix and $\boldsymbol{A}_q \in \mathcal{C}^{T_1 \times T_1}$ $(q = 1, \cdots, Q)$ represent complex Hermitian matrices, which are determined in advance. Finally, $\boldsymbol{S}(n)$ is created by the differential encoding process as follows: [7]

$$\boldsymbol{S}(n) = \boldsymbol{S}(n-1)\boldsymbol{V}(n). \tag{3}$$

The source transmits each component of $\boldsymbol{S}(n)$ in a specific time slot, spanning a total of over T_1^2 symbol durations.

The received signal block $\boldsymbol{R}_m(n)$ at the mth relay is given by

$$\boldsymbol{R}_m(n) = f_m(n)\boldsymbol{S}(n) + \boldsymbol{N}_m(n), \tag{4}$$

where $f_m(n)$ is the channel coefficient between the source and the mth relay, and $\boldsymbol{N}_m(n) \in \mathcal{C}^{T_1 \times T_1}$ is the noise matrix whose components have zero mean and a variance of $2\sigma_1^2$. By stacking the received signal blocks $\boldsymbol{R}_m(n)$ $(m = 1, \cdots, M)$ in a manner reminiscent of co-located MIMO elements, we arrive at

$$\boldsymbol{R}(n) = [\boldsymbol{R}_1^T(n) \cdots \boldsymbol{R}_M^T(n)]^T = \boldsymbol{F}(n)\boldsymbol{S}(n) + \hat{\boldsymbol{N}}(n) \tag{5}$$

where we have

$$\boldsymbol{F}(n) = \boldsymbol{f}(n) \otimes \boldsymbol{I}_{T_1} \tag{6}$$

$$\hat{\boldsymbol{N}}(n) = [\boldsymbol{N}_1^T(n) \cdots \boldsymbol{N}_M^T(n)]^T \tag{7}$$

$$\boldsymbol{f}(n) = [f_1(n) \cdots f_M(n)]^T. \tag{8}$$

Here, $\otimes$ represents the Kronecker product operation.

During the cooperation phase of Fig. 1 the relay nodes employ an *amplify-and-forward* scheme based on the concept of LDCs [5]. More specifically, the received space-time block $\boldsymbol{R}_m(n)$ at the mth relay is multiplied by a pre-assigned or randomly generated dispersion matrix $\boldsymbol{B}_m \in \mathcal{C}^{T_2 \times T_1}$ having a trace satisfying the relationship of

$$\mathrm{tr}(\boldsymbol{B}_m^H \boldsymbol{B}_m) = \frac{1}{M} \cdot \left(\frac{T_2}{T_1}\right)^2. \tag{9}$$

Then, all the M relays simultaneously transmit their space-time matrices $\boldsymbol{Z}_m(n) \in \mathcal{C}^{T_2 \times T_1}$ $(m = 1, \cdots, M)$ over T_1T_2 symbol durations. Here, the matrix $\boldsymbol{Z}_m(n)$ assigned to the mth relay is given by

$$\boldsymbol{Z}_m(n) = \nu \boldsymbol{B}_m \boldsymbol{R}_m(n), \tag{10}$$

with $\nu = \sqrt{T_1^2/E[\boldsymbol{R}_m^H \boldsymbol{R}_m]} = \sqrt{1/(1+2\sigma_1^2)}$. Here, ν is the parameter that normalizes the average total transmit power of the M number of relays to unity. We note that although the low-complexity *amplify-and-forward* scheme is considered in this paper, this arrangement may also be readily extended to the *decode-and-forward* scheme, potentially achieving a better performance at the cost of an additional complexity and delay.

Let us define the tth column of $\boldsymbol{Z}_m(n)$ as $\boldsymbol{z}_m^{(t)}(n) \in \mathcal{C}^{T_2 \times 1}$. Then the corresponding received signals $\boldsymbol{Y}^{(t)}(n) \in \mathcal{C}^{N \times T_2}$ at the input of the receiver are given by

$$\boldsymbol{Y}^{(t)}(n) = \boldsymbol{G}(n)\boldsymbol{Z}^{(t)}(n) + \boldsymbol{N}_R^{(t)}(n) \tag{11}$$

with

$$\boldsymbol{Z}^{(t)}(n) = [\boldsymbol{z}_1^{(t)}(n) \cdots \boldsymbol{z}_M^{(t)}(n)]^T, \tag{12}$$

where $\boldsymbol{N}_R^{(t)}(n) \in \mathcal{C}^{N \times T_2}$ represents the noise matrix, whose components have a zero mean and a variance of $2\sigma_2^2$. Furthermore, $\boldsymbol{G}(n) \in \mathcal{C}^{N \times M}$ are the channel coefficients between the M relays and the destination's N antenna elements. Let us define the *row*( ) operation as the vertical stacking of the rows of an arbitrary matrix. Then, by applying the *row*( ) operation to (11), we have

$$\boldsymbol{y}^{(t)}(n) = \nu \hat{\boldsymbol{G}}(n)\boldsymbol{\chi}\boldsymbol{R}^{(t)}(n) + row[\boldsymbol{N}_R^{(t)}(n)], \tag{13}$$

where

$$\hat{\boldsymbol{G}}(n) = \boldsymbol{G}(n) \otimes \boldsymbol{I}_{T_2}, \tag{14}$$

$$\boldsymbol{\chi} = diag\{\boldsymbol{B}_1, \cdots, \boldsymbol{B}_M\}, \quad (15)$$

$$\boldsymbol{R}(n) = [\boldsymbol{R}^{(1)}(n) \cdots \boldsymbol{R}^{(T_2)}(n)]. \quad (16)$$

By stacking the modified received signals $\boldsymbol{y}^{(t)}(n)$ $(t = 1, \cdots, T_2)$ which belong to the same block index n, we arrive at

$$\boldsymbol{Y}(n) = [\boldsymbol{y}^{(1)}(n), \cdots, \boldsymbol{y}^{(T_2)}(n)] = \boldsymbol{H}(n)\boldsymbol{S}(n) + \boldsymbol{N}(n), \quad (17)$$

we have

$$\boldsymbol{N}'(n) = \left[row(\boldsymbol{N}_R^{(1)}(n)), \cdots, row(\boldsymbol{N}_R^{(T_2)}(n))\right] \quad (18)$$

$$\boldsymbol{H}(n) = \nu\hat{\boldsymbol{G}}(n)\boldsymbol{\chi}\boldsymbol{F}(n) \quad (19)$$

$$\boldsymbol{N}(n) = \nu\hat{\boldsymbol{G}}(n)\boldsymbol{\chi}\hat{\boldsymbol{N}}(n) + \boldsymbol{N}'(n). \quad (20)$$

Here, the covariance matrix N_0 of the equivalent noise matrix $\boldsymbol{N}$ in (17) is given by $N_0 = (2\sigma_2^2\boldsymbol{I}_{T_2} + 2\sigma_1^2\nu^2 E[\hat{\boldsymbol{G}}\boldsymbol{\chi}\boldsymbol{\chi}^H\hat{\boldsymbol{G}}^H])$.

Finally, by multiplying both sides of Eq. (17) by $[\boldsymbol{I} + j\boldsymbol{A}(n)]$, the system equation can be rewritten without containing the channel components as follows: [7]

$$\bar{\boldsymbol{Y}}(n) = \bar{\boldsymbol{H}}(n)\boldsymbol{A}(n) + \bar{\boldsymbol{N}}(n), \quad (21)$$

where we have

$$\bar{\boldsymbol{Y}}(n) = \boldsymbol{Y}(n) - \boldsymbol{Y}(n-1), \quad (22)$$

$$\bar{\boldsymbol{H}}(n) = -j[\boldsymbol{Y}(n) + \boldsymbol{Y}(n-1)], \quad (23)$$

$$\bar{\boldsymbol{N}}(n) = \boldsymbol{N}(n)[\boldsymbol{I} + j\boldsymbol{A}(n)] - \boldsymbol{N}(n-1)[\boldsymbol{I} - j\boldsymbol{A}(n)]. \quad (24)$$

Having arrived at Eq. (21), which does not include either the source-relay or the relay-destination channel components, the destination node can detect the DLDC-encoded symbols without any channel estimation by using the high-complexity exhaustive Maximum Likelihood (ML) search. Furthermore, the linearization technique of [7] enables the application of more efficient sub-optimal detection algorithms, such as the classic successive nulling and cancelling technique reminiscent of Successive Interference Cancellation (SIC). Other design alternatives are Sphere Detection (SD) or the linear Multi-User Detection (MUD)-based interference cancellation [15], [16].

The received signals are decoded based on an iterative process, which exchanges soft information in the form of Log Likelihood Ratios (LLRs) between three Soft-Input Soft-Output (SISO) decoders, i.e. the DLDC detector, the URC decoder and the channel decoder. After the affordable number of inner and outer iterations, the estimated bits are output by the channel decoder. Furthermore, considering that the symbol durations required for the broadcast- and cooperative-phase transmissions are T_1^2 and T_1T_2, respectively, the transmission rate of our system is expressed as $R = (Q/(T_1^2 + T_1T_2)\log_2 r$.

As seen in the system description part of this section, the operations in the cooperation phase of each relay are independent of the other relays as well as of the destination node, since each relay can decide without any negotiations with the other nodes, whether it joins the cooperation phase or not. This eliminates any potential overhead and any related control based on the spontaneous decisions of each relay. In the scenario considered in this paper, where the number of vehicles belonging to a cooperating cluster changes dynamically and where the associated source-relay channel SNRs are different depending on the position of the relays, this capability of adapting the cooperation without any complex admission procedure is beneficial.

III. System Performance

In this section, we provide our performance results, comparing the effects of diverse system parameters, channel conditions and operating scenarios. As listed in Table I, the basic system parameters

TABLE I
BASIC SYSTEM PARAMETERS

(MNT_1T_2Q)	(42224)
Source-relay channels	Rician block fading channels with $K = 5$ dB
Relay-destination channels	Rayleigh block fading channels
Modulation Scheme	BPSK for each dispersion matrix
Outer channel code	RSC (2,1,2) with generator polynomials (7, 5)
Interleaver block length	200,000 bits
Number of inner iterations $I_{\rm in}$	$I_{\rm in}$ = 2
Number of outer iterations $I_{\rm out}$	$I_{\rm out}$ = 0 to 9
RSC Channel decoder	Approximate Log MAP
Weight optimization criterion	MMSE-based interference cancellation

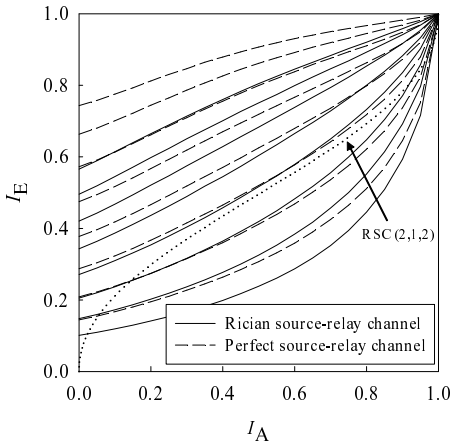

Fig. 3. EXIT curves of the two different source-relay channels. The EXIT curve of the outer code is also plotted.

are set to $(MNT_1T_2Q) = (42224)$, where each of the Q dispersion matrices uses BPSK modulation, i.e. $r = 2$. Thus, the corresponding inner code rate is 0.5 and the associated throughput is bits/s/Hz. The source employs a half-rate Recursive Systematic Convolutional (RSC) code having a constraint length of $K = 2$ and octally represented generator polynomials of (7,5) as well as two random interleavers having a length of 200,000 bits. At the destination's receiver the popular Minimum Mean Square Error (MMSE)-based interference cancellation algorithm [15] is employed for the DLDC detector and the number of the inner and outer iterations is set to $I_{\rm in}$ = 2 and $I_{\rm out}$ = 9, respectively. In line with [13], independent Rayleigh block fading channels are considered for the relay-destination channels, which remain constant over two successive block durations, i.e. our $2(T_1^2 + T_1T_2)$ symbol durations. For simplicity, the elements of the dispersion matrices $\boldsymbol{B}_m$ $(m = 1, \cdots, M)$ of each relay were generated to have random Gaussian distribution, noting that any $(T_2 \times T_1)$-element complex-valued matrices can be employed for the dispersion matrices, as long as they satisfy the norm constraint of Eq. (9).

A. EXIT chart analysis

Fig. 3 shows the EXIT curves of the two different source-relay channels, i.e. of independent Rician block-fading channels and of perfect channels, in the context of our DLDC-aided cooperative system, where the relay-destination SNR $\rho_{\rm rd}$ is gradually increased from $\rho_{\rm rd}$ = 0 dB to $\rho_{\rm rd}$ = 8 dB in steps of 1 dB. Here, the channels have a Rician factor of $K = 5$ dB and the source-relay SNR is $\rho_{\rm sr}$

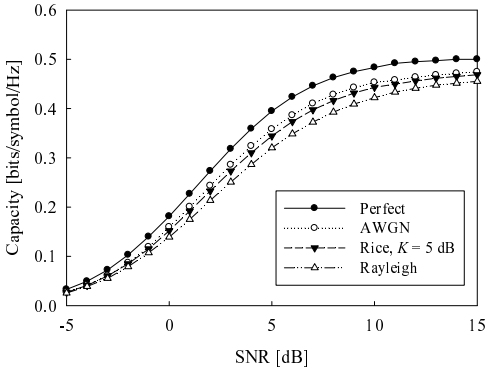

Fig. 4. Maximum achievable rate of the MMSE detector in our DLDC-aided cooperative system employing the $(MNT_1T_2Q) = (42224)$ scheme and different source-relay channels, i.e. perfect, AWGN, Rician and Rayleigh channels at the source-relay SNR of $\rho_{\rm sr}$ = 10 dB.

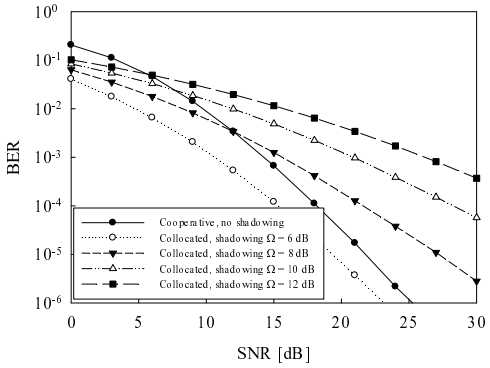

Fig. 5. Comparison of achievable BER performance of a collocated MIMO and our cooperative MIMO in the uncoded scenario. The collocated MIMO is DLDC-encoded using the parameters of $(MNTQ) = (4242)$ and experiences large-scale shadow fading associated with the standard variations of Ω = 6, 8, 10 and 12 dB.

= 10 dB, while the perfect channels assume having no information loss between the source and the relays. The EXIT curve of the RSC code employed in this paper is also plotted. As seen in Fig. 3, all the EXIT curves reach the point of perfect convergence at (I_A, I_E) = (1.0, 1.0), as a benefit of the URC code's employment. The EXIT curve of the Rician source-relay channels exhibits an open tunnel at $\rho_{\rm rd}$ = 3 dB, while that of the perfect source-relay channel facilitates an open tunnel at a 1 dB lower relay-destination SNR $\rho_{\rm rd}$. Therefore, as expected, the impairments imposed by the source-relay channel degrade the achievable performance, which is upper bounded by that recorded for perfect source-relay channels, which may also be interpreted as the perfect-relaying based *decode-and-forward* scheme's performance in the absence of decoding errors.

Furthermore, we investigated the maximum achievable rates of the four different source-relay channels, which were calculated based on our EXIT chart results. It was shown in [17] that the maximum achievable rate may be expressed as $C(\rho_{\rm rd}) = R \cdot A(\rho_{\rm rd})$, where $A(\rho_{\rm rd})$ is the area under the EXIT curves corresponding to a certain value of $\rho_{\rm rd}$. In addition to the two source-relay channels used in Fig. 3, in Fig. 4 we considered two more source-relay channels, namely independent block-fading Rayleigh and AWGN channels, while maintaining a source-relay channel SNR of $\rho_{\rm sr}$ = 10 dB.

Observe in Fig. 4 that as expected, the perfect source-relay channel exhibited the best maximum achievable rate, followed by the AWGN, Rician and Rayleigh channels. More specifically, considering the employment of the half-rate channel encoder in our system, the maximum achievable rate is attained at the relay-destination SNRs of $\rho_{\rm rd}$ = 1.5 dB, 2.2 dB, 2.4 dB and 3.0 dB for the cases of the perfect, AWGN, Rician and Rayleigh channels, respectively. In the rest of this section, we adopt the Rician source-relay channels associated with $\rho_{\rm sr}$ = 10 dB and K = 5 dB for the source-relay channels, unless noted otherwise.

B. BER performance

Fig. 5 compares the achievable BER performance of our cooperative system and that of the corresponding collocated MIMO system, where the source node of the collocated MIMO is equiped with M = 4 transmit antennas and transmits the DLDC-encoded signals to the destination's receiver without any cooperation. The other DLDC parameters of the collocated MIMO were set to $(MNTQ)$ = (4242) so that the two systems have the same overall transmission rate R. For simplicity, we assume that both systems are uncoded, i.e. use no RSC coding before the DLDC block of the transmitter

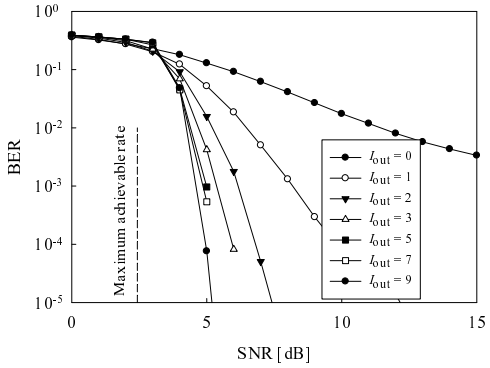

Fig. 6. BER performance of different number of outer iterations $I_{\rm out}$ in our DLDC-aided cooperative system employing the $(MNT_1T_2Q) = (42224)$ scheme and BPSK modulation for each dispersion matrix. The corresponding maximum achievable rate is also plotted.

seen in Fig. 2. We also consider Rayleigh fading source-destination channels contaminated by large-scale shadow fading [8] associated with standard deviations of Ω = 6, 8, 10 and 12 dB for the collocated MIMO system. On the other hand, in the cooperative system perfect source-relay channels and Rayleigh relay-destination channels are considered, respectively, assuming that the most appropriate relays are selected during the formation of the cooperating cluster. Observe in Fig. 5 that as expected, the BER curves of the collocated MIMO system degrade upon increasing the value of Ω. When shadowing is dominant in the collocated MIMO system, our cooperative system achieves a higher diversity gain than the collocated MIMO system.

Fig. 6 shows the achievable BER performance of our system, where the number of outer iterations $I_{\rm out}$ is varied from $I_{\rm out} = 0$ to $I_{\rm out} = 9$. The value of the corresponding maximum achievable rate derived by evaluating the area under the inner decoder's EXIT curve is also shown. Observe that upon increasing the value of $I_{\rm out}$, the achievable BER performance is significantly improved and there is no error floor in case of $I_{\rm out} \geq 2$. More specifically, the relay-destination SNR $\rho_{\rm rd}$ required for achieving BER = 10^{-5} is 3.5 dB away from the curve representing the maximum achievable rate in the case of $I_{\rm out} = 9$.

Fig. 7 shows the achievable BER performance for different source-relay SNRs $\rho_{\rm sr}$ ranging from $\rho_{\rm sr} = 0$ dB to $\rho_{\rm sr} = 20$ dB. Albeit the BER curve of $\rho_{\rm sr} = 0$ dB exhibits a BER floor in this SNR region, the performance drastically improves upon increasing the value of $\rho_{\rm sr}$.

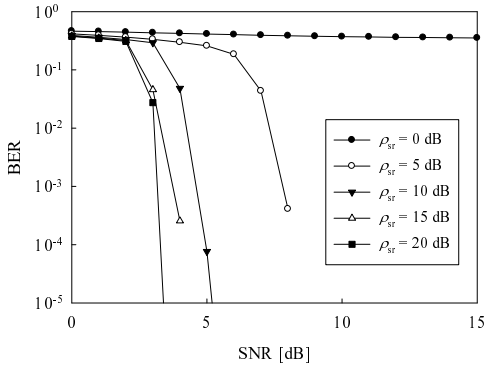

Fig. 7. BER performance for different source-relay SNRs $\rho_{\rm sr}$ ranging from $\rho_{\rm sr}$ = 0 dB to $\rho_{\rm sr}$ = 20 dB in our DLDC-aided cooperative system employing the $(MNT_1T_2Q) = (42224)$ scheme and BPSK modulation for each dispersion matrix.

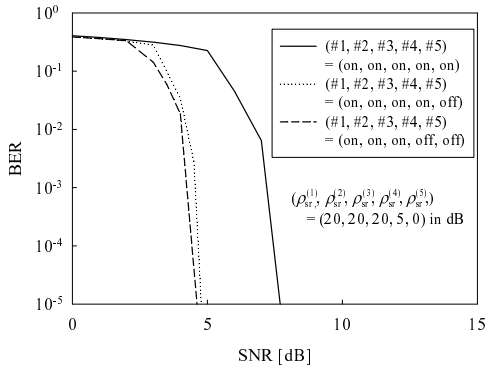

Fig. 8. Comparison of the achievable BER performance in our DLDC-aided cooperative system employing the $(MNT_1T_2Q) = (52224)$ scheme and BPSK modulation for each dispersion matrix, when the activation of the relays is changed. The source-relay SNRs are set to $(\rho_{\rm sr}^{(1)}, \cdots, \rho_{\rm sr}^{(5)})$ = (20, 20, 20, 5, 0) in dB.

This result implies that when the cooperating cluster includes relays that suffer from a low source-relay SNR, the appropriate selection of the cooperating relays is important in order to avoid the associated performance deterioration.

In Fig. 8 we investigate the effect of spontaneous deactivations of the cooperating relays in the scenario of the $(MNT_1T_2Q) = (52224)$ scheme, where all of the M = 5 relays experience different source-relay SNRs, which were set to $(\rho_{\rm sr}^{(1)}, \cdots, \rho_{\rm sr}^{(5)})$ = (20, 20, 20, 5, 0) in dB. Since in our system each relay can decide on joining or leaving the cooperating cluster without consulting the others, spontaneous cooperation can be readily established by introducing a source-relay SNR threshold as our activation criterion. Fig. 8 compares three schemes. The first is the scenario, where all of the M = 5 relays are activated. In the second scenario, the relay having $\rho_{\rm sr}^{(5)}$ = 0 dB is deactivated. In the last scenario, the two lowest-quality relays having SNRs of $\rho_{\rm sr}^{(4)}$ = 5 dB and $\rho_{\rm sr}^{(5)}$ = 0 dB are deactivated. Observe in Fig. 8 that at the BER = 10^{-5} the two curves that correspond to deactivating the relay associated with $\rho_{\rm sr}^{(5)}$ = 0 dB exhibit a 3 dB better performance than that representing the 'no deactivation' scenario. Thus, the incorporation of the threshold-based activation criterion was found to be effective in this scenario.

IV. Conclusions

In this paper, we proposed a DLDC-encoded cooperative transmission scheme suitable for VANETs, which is capable of striking a flexible diversity-multiplexing gain tradeoff, while requiring no channel estimation at any of the relay and destination nodes. A sophisticated LDC-based relaying scheme was employed, which allows each relay to decide autonomously, whether to join the cooperating cluster without any negotiations with the other nodes. Based on the serially concatenated turbo coding principle, the source node is constituted by the channel encoder, URC encoder and DLDC-based mapper. The destination's receiver decodes the received signals iteratively, exchanging soft information between the DLDC demapper, the URC decoder and the channel decoder. Our simulation results demonstrated that at the BER = 10^{-5} the proposed cooperative scheme attained a good BER performance within 2.8 dB of the maximum achievable rate curve and outperformed the corresponding collocated MIMO system in the presence of large scale fading. We also investigated the effects of different source-relay channels, i.e. that of the perfect, AWGN, Rician and Rayleigh channels. Additionally, the proposed spontaneous cooperation of the relays required the introduction of an appropriate source-relay SNR threshold for improving the attainable performance.

References

[1] H. Hartenstein and K. Laberteaux, "A tutorial survey on vehicular ad hoc networks," *IEEE Commun. Mag.*, vol. 46, no. 6, pp. 164–171, 2008.

[2] L. Hanzo, M. Münster, B. Choi, and T. Keller, *OFDM and MC-CDMA for Broadband Multi-User Communications, WLANs and Broadcasting*. John Wiley and IEEE Press, 2003.

[3] S. Alamouti, "A simple transmit diversity technique for wireless communications," *IEEE J. Sel. Areas Commun.*, vol. 16, no. 8, pp. 1451–1458, 1998.

[4] B. Hochwald and W. Sweldens, "Differential unitary space-time modulation," *IEEE Trans. Commun.*, vol. 48, no. 12, pp. 2041–2052, 2000.

[5] B. Hassibi and B. Hochwald, "High-rate codes that are linear in space and time," *IEEE Trans. Inform. Theory*, vol. 48, no. 7, pp. 1804–1824, 2002.

[6] N. Wu and L. Hanzo, "Near-capacity irregular convolutional-coding aided irregular precoded linear dispersion codes," *IEEE Trans Veh. Technol.*, vol. 58, no. 6, 2009, to appear.

[7] B. Hassibi and B. Hochwald, "Cayley differential unitary space-time codes," *IEEE Trans. Inform. Theory*, vol. 48, no. 6, pp. 1485–1503, 2002.

[8] W. Jakes and D. Cox, *Microwave Mobile Communications*. John Wiley and IEEE Press, 1994.

[9] V. Erceg, S. Ghassemzadeh, M. Taylor, D. Li, and D. Schilling, "Urban/suburban out-of-sight propagation modeling," *IEEE Commun. Mag.*, vol. 30, no. 6, pp. 56–61, 1992.

[10] J. Laneman and G. Wornell, "Distributed space-time-coded protocols for exploiting cooperative diversity in wireless networks," *IEEE Trans. Inform. Theory*, vol. 49, no. 10, pp. 2415–2425, 2003.

[11] R. Nabar, H. Bolcskei, and F. Kneubuhler, "Fading relay channels: performance limits and space-time signal design," *IEEE J. Sel. Areas Commun.*, vol. 22, no. 6, pp. 1099–1109, 2004.

[12] Y. Jing and B. Hassibi, "Distributed space-time coding in wireless relay networks," *IEEE Trans. Wireless Commun.*, vol. 5, no. 12, p. 3524, 2006.

[13] Y. Jing and H. Jafarkhani, "Distributed differential space-time coding for wireless relay networks," *IEEE Trans. Commun.*, vol. 56, no. 7, pp. 1092–1100, 2008.

[14] Y. Tadokoro, K. Ito, J. Imai, N. Suzuki, and N. Itoh, "Advanced transmission cycle control scheme for autonomous decentralized TDMA protocol in safe driving support systems," in *IEEE Intell. Vehicles Symp. 2008*, Eindhoven, Netherlands, 4-6 June 2008, pp. 1062–1067.

[15] X. Wang and H. Poor, "Iterative (turbo) soft interference cancellation and decoding for coded CDMA," *IEEE Trans. Commun.*, vol. 47, no. 7, pp. 1046–1061, 1999.

[16] S. Sugiura, S. Chen, and L. Hanzo, "Reduced-complexity iterative Markov chain MBER detection for MIMO systems," *IEEE Signal Processing Letters*, vol. 16, no. 3, pp. 160–163, 2009.

[17] M. Tüchler, "Design of serially concatenated systems depending on the block length," *IEEE Trans. Commun.*, vol. 52, no. 2, pp. 209–218, 2004.